Bulgarian Chemical Communications, Volume 48, Number 2 (pp. 238 – 243) 2016

Nickel doping effect on the photocatalytic activity of TiO_2/SiO_2 nanocomposite

B. Khodadadi

Department of Chemistry, University of Qom, Qom, Iran

Received January 24, 2015, Revised July 31, 2015

TiO_2/SiO_2 and TiO_2/SiO_2/Ni nanocomposite powders were prepared by a sol-gel technique. Moreover, different concentrations of dopant were added to investigate the effect of the metal doping effect. Structures were characterized by IR spectroscopy, Scanning Electron Microscopy (SEM), Energy Dispersive Analytical X-Ray (EDAX) and X-Ray Diffraction (XRD) methods. Moreover, the absorption coefficients of the samples were analyzed by Tauc's approach and the direct band gaps also were calculated. The photocatalytic activity of all the samples was investigated under UV irradiation in an aqueous medium. The results revealed that metal doping plays an important role in decreasing the particle size. Furthermore, photocatalytic activity improves in the presence of a dopant.

Keywords: Sol-Gel, Nanocomposite, Photocatalytic activity, TiO_2/SiO_2/Ni

INTRODUCTION

Photocatalytic and self-cleaning properties have already become a very interesting subject for researchers and can be used for practical applications regarding environmental decontamination. These properties depend on the relationship between photocatalysis and hydrophilicity, which causes more effective cleaning over the surfaces and is useful for decomposition of organic contaminants. TiO_2 is one of the best materials for self-cleaning purposes due to its thermostability and photocatalytic properties [1,2].

Recently, many researchers have reported replacing TiO_2 by the TiO_2/SiO_2 catalyst, which is an advanced material for self-cleaning and photocatalytic properties, since TiO_2/SiO_2 exhibits different surface chemical and photochemical properties compared to TiO_2 [3, 4]. In order to improve the efficiency of the photocatalytic activity, the TiO_2/SiO_2 catalyst can be modified by the addition of various modifiers, such as metals or metallic oxides by various methods [5-8].

The metal doping process can be performed by the sol–gel method or restricted to the surface by metal deposition. Proportional abundance and low-cost properties are reasons for choosing Nickel in this process [8-11]. The photocatalytic properties are related to the surface structure of the nanocomposite powder [12]. On the other hand, organic polymers are used to prevent agglomeration of TiO_2 powder and modify its photocatalytic activity [13, 14].

Consequently, in this work, we have synthesized TiO_2/SiO_2 nanocomposites, doped with Ni. Moreover, we have investigated the effects of the molar ratio of the dopant on the particle size, structure and photocatalytic activity.

EXPERIMENTAL

Materials and Equipment

Titanium tetra isopropoxide (TTIP) (AR analytical grade, Merck Chemical Company) was used as the titanium source for the preparation of the TiO_2 photocatalysts. Nickel (II). 6 H_2O, Hydroxypropyl cellulose (HPC), HNO_3, SiO_2 colloid solution, absolute ethanol were purchased from the Merck Chemical Company. XRD measurements were performed using a Philips X' Pert PRO MPD diffractometer with CuK_α radiation from 10 to 80 (2θ) at room temperature. The morphology and microanalysis of the samples were observed by a scanning electron microscope (SEM, SEM-4100, Jeol). Ultraviolet-visible (UV-Vis) absorption spectra were obtained by means of a Varian Carry 300. FT-IR spectra were obtained via KBr pellets in the range 500 to 4000 cm^{-1} using a Thermo Nicolet 870 FT-IR Nexus spectrophotometer.

Preparation of the Samples

All samples were prepared by the Sol-Gel technique using the following procedure:

Preparation of sample 1 (TiO_2/SiO_2 nanocomposite)

A: Preparation of solution I: 0.2 g of (HPC) was added to absolute ethanol and stirred until complete dissolution was achieved. Then, TTIP was

* To whom all correspondence should be sent:
E-mail: bkhodadadi98@yahoo.com; Khodadadi@qom.ac.ir

dissolved in this solution (with a molar ratio TTIP/ethanol = 1/75).

B: Preparation of solution II: HNO_3, deionized water and SiO_2 were dissolved in absolute ethanol (with a molar ratio ethanol /HNO_3/H_2O/SiO_2 = 43/0.2/1/30).

C: Preparation of the TiO_2/SiO_2 nanocomposite: Solution II was added dropwise into solution I and vigorously stirred for 30 min at room temperature. The obtained transparent colloidal suspension was sonicated for 30 min. and aged for 48 h to form a gel. The sample was dried in an oven at 50°C and ultimately calcinated at 500°C for 4 hours.

*Preparation of samples **2**, **3**, **4**, and **5** (TiO_2/SiO_2/Ni nanocomposite)*

A: Preparation of solution I: Solution A was prepared exactly as sample 1.

B: Preparation of solution II: HNO_3, deionized water and SiO_2 were dissolved in absolute ethanol (with a molar ratio ethanol /HNO_3/H_2O/SiO_2 = 43/0.2/1/30) and then several concentrations of Ni $(NO_3)_2$ (0.1, 0.3, 0.6) and 1% W/W Ni $(NO_3)_2$/ SiO_2 were added to solution II.

C: Preparation of TiO_2/SiO_2/Ni nanocomposite: Solution II was added dropwise into solution I and vigorously stirred for 30 min at room temperature. The obtained transparent colloidal suspension was sonicated for 30 min. and aged for 48 h to form a gel. The sample was dried in an oven at 50°C and ultimately calcinated at 500°C for 4 hours.

All the above steps have been summarized in a chart in Fig. 1.

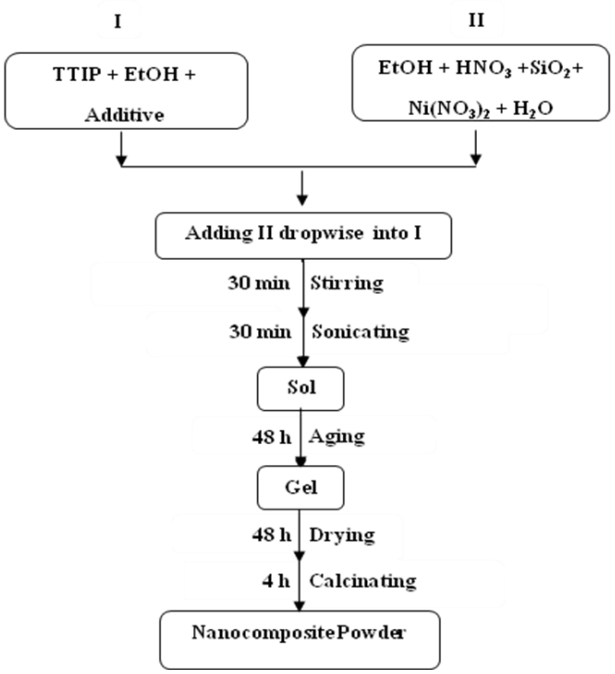

Fig. 1. Sample preparation chart

RESULTS AND DISCUSSION

FT-IR spectroscopy

Fig. 2 presents the FT-IR spectra of the samples investigated. According to these results, in all samples, wide absorption bands were observed around 3100-3700 cm^{-1}, which can be attributed to the OH stretching vibration of the surface hydroxyl group. Hydroxyl bands (3100-3700 cm^{-1}) appeared due to a great amount of propanol present during the hydrolysis of TTIP [15-20]. Moreover, because of the physically adsorbed water and hydroxyl group, absorption bands were observed around 1635 cm^{-1} [19,20].

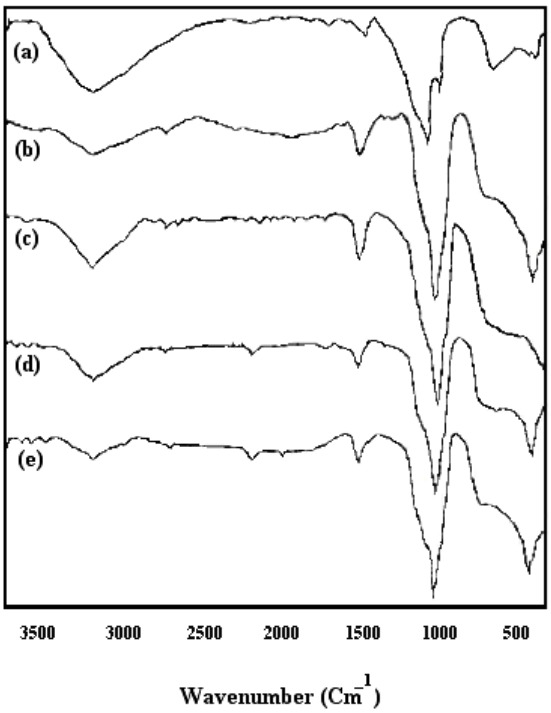

Fig. 2. FT-IR spectra of the sample sols. (a)Sample 1, (b)Sample 2, (c)Sample 3, (d)Sample 4 and (e) sample 5.

The bands at 1117 cm^{-1} in the samples correspond to an asymmetric stretching vibration of the Ti-O bands [17-21] and the ones at 1073 cm^{-1} are due to the symmetrical vibration of the Si-O-Si bands [20-22]. The FT-IR spectra show silicate absorptions at 789, 467 and 464 cm^{-1}, which can be assigned to Si–O–Si bending and stretching vibrations [22-24]. The peak at 602 cm^{-1} can be assigned to a symmetric stretching vibration of the Ti–O–Ti group [22-25]. Furthermore, a band was observed at 2366 cm^{-1}, which can be assigned to Ni–TiO_2–SiO_2 [5, 7]. Exhibited broad peaks in the range of 400–1000 cm^{-1} have contributions from the anatase phase [21-24].

XRD analysis

X-ray diffraction (XRD) analysis was employed to determine the crystallite phase and crystallinity of the samples and the results have been shown in Fig. 3.

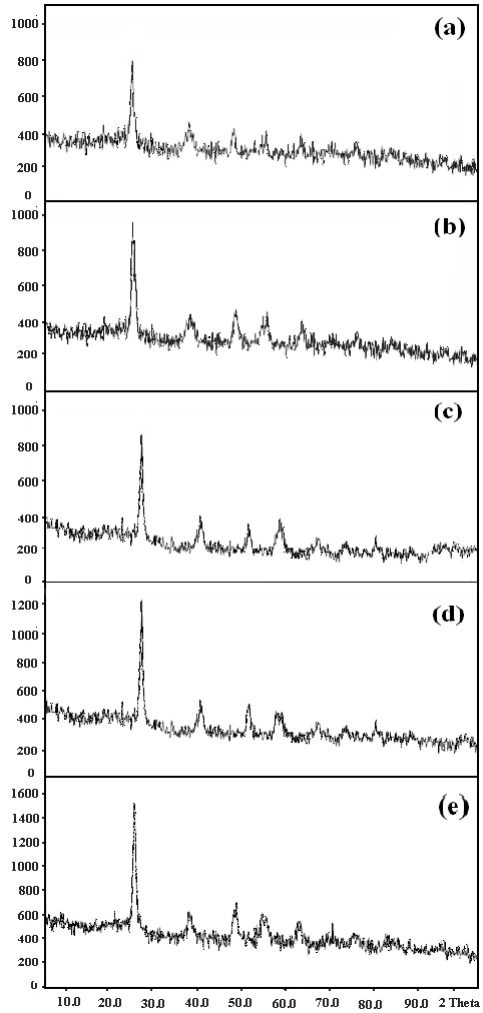

Fig. 3. XRD patterns of sol-gel synthesized TiO_2/SiO_2. (a) Sample 1, (b) Sample 2, (c)Sample 3, (d) Sample 4 and (e) Sample 5.

According to the XRD evaluation, the diffraction patterns of each sample are well in agreement with the anatase phase (the base peak in the range of $20<2\theta<30$ is evidence of an anatase phase). Sample 1, without Nickel shows less of an anatase structure than other samples. The XRD results reveal that the samples show an anatase phase more than sample 1 after Ni doping and this leads one to conclude that metal doping is effective on anatase phase formation. Additionally, there is no notable shift of all diffraction peaks between the samples, confirming the successful doping of Ni into the lattice. However, the intensity of the diffraction peaks becomes higher with increasing Ni concentration.

Scanning Electron Microscopy (SEM) and EDAX analysis

All samples were identified by Scanning Electron Microscopy (SEM) analysis and their images are presented in Fig. 4. According to the images, in all samples, the nanoparticles are relatively uniform, global and slightly agglomerated. It is remarkable that the particle size decreases and becomes monotonous and particle distribution becomes narrow with the increase in Ni^{2+} doping concentration. This clearly reveals that the Nickel ion decreases the grain size. EDAX analysis has revealed that TiO_2, SiO_2 and Ni are present in all the samples.

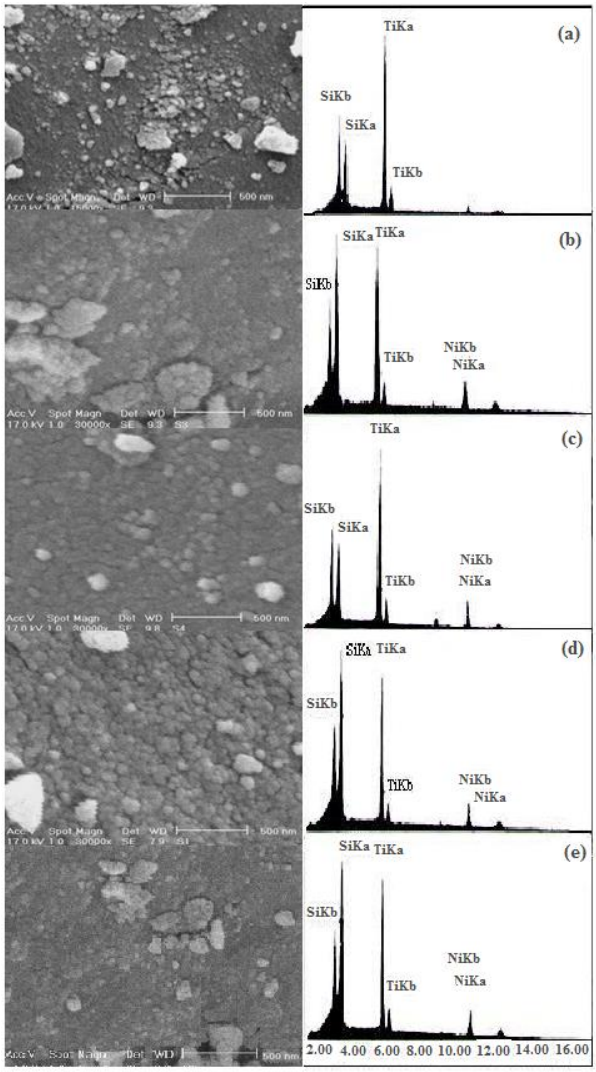

Fig. 4. SEM images for the sample powders. (a) Sample 1, (b) Sample 2, (c) Sample 3, (d) Sample 4 and (e) Sample 5.

UV–Visible spectra and Band gap calculation

UV–Vis diffuse reflectance spectroscopy was carried out to investigate the optical properties of the samples and the results are shown in Fig. 5. It

can be clearly seen that the maximum of the absorbance band shifts slightly toward a higher wavelength due to Ni doping and sample 5 shows huge absorption intensity in the higher wavelength region.

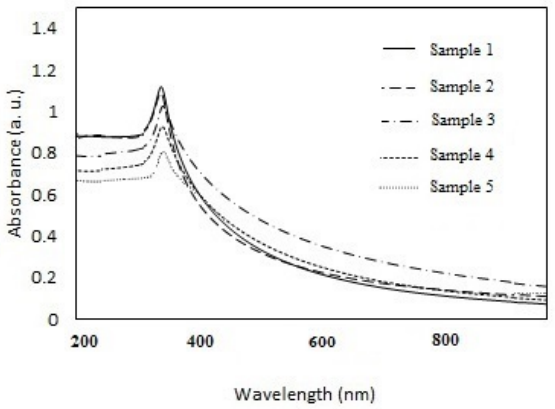

Fig. 5. Uv–vis spectra of the samples.

The absorption coefficients of the samples are analyzed utilizing a Tauc approach [26] and the direct band gap is calculated using the following equation:

$$\alpha = C\,(h\nu - E_g^{bulk})^2 / h\nu$$

Where α is the absorption coefficient, C is a constant, hν is the photon energy and E_g bulk is the band gap.

Table 1 shows the calculated band gap of the samples. According to these results, band gap decreases with doping Ni and increasing concentration of dopant. Fig. 6 shows the Tauc plots of the samples. Extrapolation of the linear region of the Tauc plot gives a band gap. From Fig. 6, it can be seen that, compared with sample 1, the band gap of the samples with a dopant decreases. It can be seen that the band gap slightly decreases with the increase in Ni concentration and these results are consistent with the Uv-Vis spectra.

Table1. Calculated band gap of the samples

sample	Mole ratio ([dopant]/[TiO_2])%	Band gap(eV)
1	-------	3.05
2	0.1	2.97
3	0.3	2.93
4	0.6	2.86
5	1	2.82

Evaluation of the photocatalytic activity of the samples

To investigate the photocatalytic activity of the samples and the effect of metal doping on the photocatalytic activity, several solutions of methyl orange (with a concentration of 5 mgL^{-1}) in deionized water were selected as pollutant solutions for photodegradation. These solutions were set in the vicinity of a nano photocatalyst powder (0.5 g powder in 1L solution) and then placed in the dark for 24 h in order to eliminate the absorptive effect of the solution in the catalyst. Finally, the solutions were placed in the photoreactor and methyl orange concentration change was recorded by UV spectroscopy. This photoreactor system consisted of a cubic borosilicate glass reactor with an effective volume of 1000 mL, a cooling water jacket and a 15W UV lamp (Osram) with a quartz cover positioned inside the solution used as a UV light source. The reaction temperature was kept at 25 °C using cooling water.

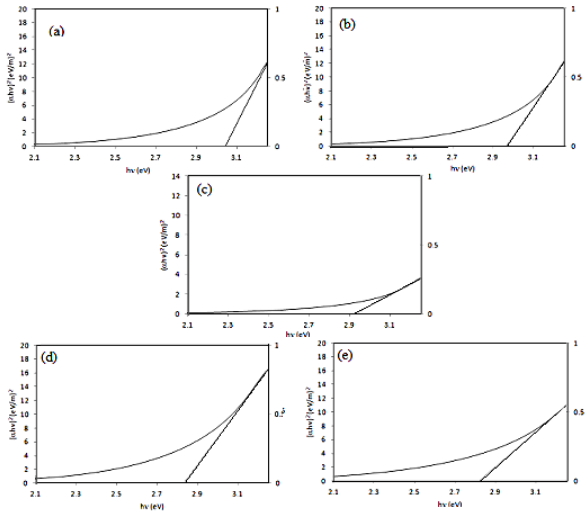

Fig. 6. The Tauc plots of samples. (a) Sample 1, (b) Sample 2, (c) Sample 3, (d) Sample 4 and (e) Sample 5.

The results are shown in Fig. 7.

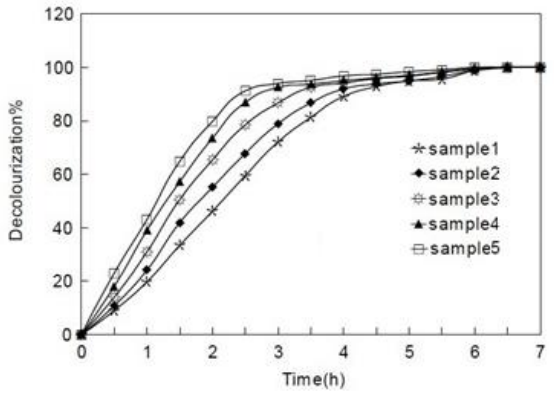

Fig.7. Decolourization percentage of Methyl orange solution under UV radiation

According to these results, the photocatalytic activity increases with the application of metal doping. It seems that the better photocatalytic activity responses after Ni doping are due to the charge-transfer transition from the electron donor levels formed by the 3d orbital's of doped Ni^{2+} to

the conduction bands of the host materials [27]. Sample 5 (containing 1% Ni) has the highest activity in comparison with other samples. Therefore, the good photocatalytic ability of this sample can be attributed to the smaller particle size, porosity and less agglomerated nanostructure.

CONCLUSION

This research has verified that the photocatalytic activity of TiO_2/SiO_2 nanocompsite powder can be improved using metal doping. All samples have been prepared by the sol–gel method and HPC has been used as a modifier. SEM pictures have revealed that the particle size of the nanocomposite powder with 1% Ni was smaller than that of the other samples. Furthermore, the XRD pattern confirmed that the formation of the anatase structure in this sample is better than in other samples. UV–Vis diffuse reflectance spectroscopy showed a red shift with doping and 1% Ni was more effective than other concentrations. Moreover, the absorption coefficients of the samples were analyzed by the Tauc approach and the calculations confirmed that the application of dopands and dopant concentrations affect the band gap. The photocatalytic activity of the samples was examined for degradation of methyl orange in water under UV irradiation in a batch reactor. The results revealed that the photocatalytic activity of the nanocomposites increased in the presence of Nickel and according to other results; the sample with 1% Ni exhibited the best photocatalytic activity.

REFERENCES

1. C. Euvananont; C. Junin; K. Inpor; P. Limthongkul, C. Thanachayanont, *Ceram. Int.*, **34**, 1067 (2008).
2. S.Neatu; V.I. Parvulescu; G. Epure; N. Petera; V. Somoghi; G. Ricchiardi; S. Bordiga, A. Zecchina, *J. Appl. Catal. B.*, **91**, 546 (2009).
3. B. Braconnier; C.A. Paez; S. Lambert; C. Alie; C. Henrist; D. Poelman; J. Pirard; R. Cloots, B. Heinrichs, *Microporous Mesoporous Mater.*, **122**, 247 (2009).
4. Z. Liu; X. Zhang; T. Murakami, A. Fujishima, *Sol. Energy Mater. Sol. Cells.*, **92**, 1434 (2008).
5. T. A. Egerton, I. R. Tooley *J. Phy. Chem. B.*, **108**. 5066 (2004).
6. A. Fujishima; T. Rao, D. Tryk. *J. Photochem. Photobiol. C. Photochem. Rev.*, **1**, 1 (2000).
7. X. Fu; L. A. Clark; Q. Yang, M. A. Anderson, *J. Environ. Sci. Tech.*, **30,** 647 (1996).
8. X. Deng; Y. Yue, Z. Gao, *J. Appl. Catal. B.*, **39**, 135 (2002).
9. H. Hayashi, K. Torii, *J. Mater. Sci.*, **12**, 3671 (2002).
10. Y. Li; N. H. Lee; D. S. Lee; D. S. Hwang; J. S. Song; E. G. Lee, S. J. Kim, *J. Langmuir*, **20**, 10838 (2004).
11. R. Rodriguez; S. J. Sandoval; M. Estevez, S. Vargas, *J. Non-Cryst. Solids*, **351**, 167 (2005).
12. H. Imai, H. Hirashima, *J. Am. Ceram. Soc.*, **82**, 2301 (1999).
13. S. Liu; N. Jaffrezic, C. Guillard, *J. Appl. Surf. Sci.*, **255**, 2704 (2008).
14. M.M. Mohamed; T.M. Salama, T. Yamaguchi, *J. Colloids Surf.*, **207**, 25 (2002).
15. K. Guan, *J. Surf. Coat. Tech.*, **191**, 155 (2005).
16. M. Houmard; D. Riassetto; F. Roussel; A. Bourgeois; G. Berthome; J.C. Joud, M. Langlet, *J. Appl. Surf. Sci.*, **254**, 1405 (2007).
17. J. Ovenstone, *J. Mater. Sci.*, **36**, 1325 (2001).
18. M.P. Zheng; M. Gu; Y. Jin and G. Jin, *J. Mater. Sci. Eng. B.*, **77**, 55 (2000).
19. G. Zhao; Q. Tian; Q. Liu, G. Han, *J. Surf. Coat. Tech.*, **198**, 55 (2005).
20. K.M. Parida, N. Sahu, *J. Mol. Catal. A: Chem.*, **287**, 151 (2008).
21. M.P. Zheng; M.Y. Gu; Y.P. Jin; H.H. Wang,; P.F. Zu; P. Tao, J.B. He, *J. Mater. Sci. Eng. B.*, **87**, 197 (2001).
22. J. Jiao; Q. Xu, L. Li, *J. Colloid Interface Sci.*, **316** , 596 (2007).
23. M. Houmard; D. Riassetto; F. Roussel; A. Bourgeois; G. Berthome; J.C.Joud, M. Langlet, *J. Surf. Sci.*, **602**, 3364 (2008).
24. P. Aberomand Azar; S.Moradi Dehaghi; S. Samadi; S. Kamyar, M. Saber Tehrani, *Asian J. Chem.*, **22**, 1619 (2010).
25. B. Khodadadi; M. Sabeti; S. Moradi; P. Aberomand Azar, S. Raies Farshid, *J. Appl. Chem. Res.*, **20**, 36 (2012).
26. H. Fu; C. Pan; W. Yao, Y. Zhu, *J. Phys. Chem., B.* **109**, 22432 (2005).
27. R. Niishiro; H. Kato, A. Kudo, ***J.*** *Phys. Chem. Chem. Phys.*,**7**, 2241 (2005).

ЕФЕКТ НА ДОТИРАНЕ С НИКЕЛ ВЪРХУ ФОТОКАТАЛИТИЧНАТА АКТИВНОСТ НА НАНОКОМПОЗИТИ ОТ TiO_2/SiO_2

Б. Ходадади

Департамент по химия, Университет в Кум, Кум, Иран

Постъпила на 24 януари, 2015 г.; коригирана на 31 юли, 2015 г.

(Резюме)

Приготвени са прахови нанокомпозити от TiO_2/SiO_2 и $TiO_2/SiO_2/Ni$ по зол-гел метода. Освен това са добавени различни концентрации на примеси са да се изследва дотиращия ефект на металите. Структурите са установени с ИЧ-спектроскопия, сканираща електронна микроскопия (SEM), дисперсионна аналитична рентгенова дифракция (EDAX) и рентгенова дифракция (XRD). Абсорбционните коефициенти на пробите са анализирани по подхода на Tauc и са изчислени директно забранените зони. Изследвана е фотокаталитичната активност на всички образци под ултравиолетово облъчване във водна среда. Резултатите показват, че дотирането с метали играе важна роля за намаляване размерите на частиците. Фотокаталитичният ефект се подобрява при дотиране.